

IR 40 03056 ✓

1.

3. Workshop on "Gases in strong rotation".  
Rome, Italy, March 27 - 30, 1979.  
CEA - CONF 4686

DISCUSSION OF VARIOUS FLOW CALCULATION  
METHODS IN HIGH-SPEED CENTRIFUGES

INIS

By P. LOUVET and C. CORTET

SCPL

DSI

A B S T R A C T

The flow in high-speed centrifuges has been studied in the frame of linearized theory for long years. Three different methods have been derived for viscous compressible flow with small Ekman numbers and high Mach numbers :

- Numerical solution of flow equation by finite element method and Gaussian elimination (CENTAURE Code),
- Boundary layer theory using matched asymptotic expansions,
- The so called eigenfunction method slightly modified.

The mathematical assumptions, the easiness and the accuracy of the computations are compared.

Numerical applications are performed successively for thermal countercurrent centrifuges with or without injections.

## 1. - INTRODUCTION

Rapidly rotating gas flow is of high interest from the basic fluid mechanics point of view as well as from an improvement of centrifuges for the separation of uranium isotopes. As no attempt to measure the velocity profiles have succeeded at high speeds of rotation, the emphasis has been set since a long time on calculation methods.

In a rotating container, the classical equilibrium state of isothermal rigid rotation can be perturbed slightly by prescribing a proper temperature distribution on the bounding walls, by scoops or by inlets and outlets. As the perturbation is weak (small Rossby number) the motion can be investigated by linearizing the equations of the flow /1,2/ around the equilibrium state. The flow in a  $UF_6$  centrifuge is a high Mach number flow, dominated by the Coriolis force, which means that the Boussinesq approximation does not apply. Here, we restrict ourselves mainly to the methods of resolution of the linearized system, which can be classified a priori in three kinds : the so-called eigenfunctions method, boundary layer analysis and numerical methods; simple one-dimensional solutions are omitted because they are too unrealistic (see for example RATZ /3/ ).

Historically, the first non trivial attempts were carried out in terms of eigenfunctions expansions by STEENBECK /4 / , PARKER and MAYO /5/, SOUBBARAMAYER /6/ . Some improvements were performed for high speed centrifuges by GING /7/ and BROUWERS /8/ in terms of asymptotic analysis. Here we will try to derive a complete consistent solution matched with the end caps. Later, the boundary layer analysis and matched asymptotic expansion methods has been used to seek solutions. Several authors (MATSUDA & al /9,10 / , BARK /11,12 / , LOUVET and DURIVault /13,14,15/ , BROUWERS /8/) have investigated with various assumptions the corrections due to compressibility. Our method /13/ , which consists in using matched asymptotic expansions in powers of the Ekman number, setting the relative order of the Mach and Ekman numbers in the Stewartson or detached layers, will be considered here for comparison.

In the last five years, considerable efforts have been spent on developing big computer programs : the linearized time dependent equation have been solved by LOPEZ /16,17 /and the corresponding non-linear problem

by KAI /18/ , both by finite difference method. The time independent equations have been solved by LA HARGUE /19/ by finite element method. The first iteration (linear run) of this last work will be used here.

The purpose of the present work is to compare the mathematical assumptions, the easiness and accuracy of these three methods.

## 2. - FUNDAMENTAL EQUATIONS

### 2.1. - Fundamental equations

We consider the steady motion of a compressible viscous gas in a cylinder of radius  $R$  and height  $2h$ , rotating about its axis with a constant angular velocity  $\omega$  (fig.1). Our analysis is performed on the basis of the following assumptions :

- the flow is axisymmetric  $\partial/\partial\theta = 0$
- the gaz is perfect and its transport coefficients are constant
- the gravitational acceleration is negligibly small compared to the centrifugal acceleration
- the shape factor  $\beta = h/R$  is of the order unity

The rigid unperturbed rotation state (subscript 0) is given by :

$$V = \omega r ; \quad W = 0, \quad U = 0$$

$$\frac{\rho_0(r)}{\rho_0(0)} = \frac{p_0(r)}{p_0(0)} = e^{S^2 r^2}, \quad T = T_0 \quad (1)$$

where  $r$  is the dimensionless radial coordinate,  $p$  the pressure,  $\rho$  the density,  $U, V, W$  the radial, azimuthal and axial components of velocity and  $S$  the speed ratio

$$S = \omega R \left( 2R_0 T_0 / M \right)^{-1/2} = \sqrt{\frac{\gamma}{2}} \mathcal{M} \quad (2)$$

where  $R$  is the gas constant,  $T$  the temperature,  $M$  the molecular mass,  $\gamma$  the heat specific ratio and  $\mathcal{M}$  the Mach number. In order to investigate the perturbed motion, we proceed to the change of variables :

$$\begin{aligned}
 w &= \frac{W}{\delta \omega R}, \quad u = \frac{U}{\delta \omega R}, \quad v = \frac{V}{\delta \omega R} - \frac{r}{\delta} \\
 \uparrow &= \frac{P}{\delta \rho_0(r)} - \frac{1}{\delta}, \quad \rho = \frac{\rho^*}{\delta \rho_0(r)} - \frac{1}{\delta} \\
 T &= \frac{T^*}{\delta T_0} - \frac{1}{\delta}
 \end{aligned} \quad (3)$$

The dimensionless number  $\delta$  analogous to a Rossby number denotes the importance of the perturbation. The set of Navier-Stokes equations including energy equation supplemented by an equation of state is the basic system of the problem. In this system, then terms of order  $\delta$  are neglected in front of terms of order unity, the linearization leads to a much simpler system, in the rotating frame (omitting viscous forces induced by compressibility) :

$$\frac{\partial w}{\partial z} + \frac{1}{r} L(u) = 0 \quad (4)$$

$$\frac{1}{2s^2} \frac{\partial k}{\partial z} = 2\varepsilon \Delta w \quad (5)$$

$$\frac{1}{2s^2} \frac{\partial k}{\partial r} - 2v + rT = 2\varepsilon \Delta u \quad (6)$$

$$u = \varepsilon \left( \Delta v - \frac{v}{r^2} \right) \quad (7)$$

$$S^2 ru + \frac{\varepsilon}{Pr} \frac{\gamma-1}{\gamma} \Delta T = 0 \quad (8)$$

$$\uparrow = \rho + T \quad (9)$$

where  $L = \frac{\partial}{\partial r} + 2s^2$ ,  $z = \frac{z}{R}$  is the dimensionless axial coordinate,  $\varepsilon = \mu / 2\rho_0(r)\omega R^2$  the Ekman number,  $Pr = \mu C_p / k$  the Prandtl number, and  $\vec{u} = (u, v, w)$  the relative velocity.

Typical values reads at high speed

$$\varepsilon(R) \approx 10^{-8} \text{ to } 10^{-9} \ll 1$$

$$s^2 = 10 \text{ to } 50 \text{ so that } (\gamma-1)S^2 = O(1) \quad (10)$$

$$\gamma-1 = 0.065$$

$$Pr \approx 1, \quad \beta \sim 5, \quad \delta \approx 0 \text{ to } 5 \cdot 10^{-2} \ll 1$$

## 2.2. - Boundary conditions

The usual zero velocity condition is taken at the wall of the centrifuge in absence of inlet or outlet. Otherwise, the axial velocity is equal to the inlet or outlet velocity ; these inlets and outlets can be approximated by sources and sinks in first approximation in order to calculate detached layers. In the case treated for comparison the walls are assumed perfectly conducting. Their temperature is prescribed to be  $T_w(z)$  for the side wall and  $T_{f_1}(r)$  and  $T_{f_2}(r)$  for the covers. The boundary conditions reads :

$$\begin{aligned} \text{on the side wall : } r = 1, \forall z \\ T = T_w(z), \quad u = v = w = 0 \end{aligned} \quad (11)$$

$$\begin{aligned} \text{on the top cover : } z = \beta \\ T = T_1(r), \quad u = v = 0 \\ w = \begin{cases} 0 & \text{wall} \\ w_{i,z}(r) & \text{for the } i^{\text{th}} \\ & \text{inlet or outlet} \end{cases} \end{aligned} \quad (12)$$

$$\begin{aligned} \text{on the bottom cover : } z = -\beta \\ T = T_2(r), \quad u = v = 0 \\ w = \begin{cases} 0 & \text{wall} \\ w_{i,z}(r) & \text{for the } i^{\text{th}} \\ & \text{inlet or outlet} \end{cases} \end{aligned} \quad (13)$$

## 3. - MATCHED ASYMPTOTIC EXPANSIONS

3.1. - The details of the method and of the solution are given in /13/. The cylinder is split into different layers (fig.1). The Ekman number appears as a singular parameter in the Navier-Stokes equations. An uniform approximate solution is found by matched asymptotic expansion method. The outer expansion of a quantity  $g$

$$g(r, z, \varepsilon) = g^{(0)}(r, z) + \varepsilon^{1/2} g^{(1)}(r, z) + \dots \quad (14)$$

corresponds to the main inner flow (fig.1). Two inner expansions which corresponds to the boundary layers called the Ekman layers, of thickness  $\varepsilon^{1/2}$ , along the top and bottom cover, read

$$g(r, z, \varepsilon) = \bar{g}(r, \zeta, \varepsilon) = \bar{g}^{(0)}(r, \zeta) + \varepsilon^{1/2} \bar{g}^{(1)}(r, \zeta) \quad (15)$$

where  $\zeta$  is the inner variable  $\zeta = \frac{z \pm \beta}{\varepsilon^{1/2} r}$  on the cover  $\zeta = \mp \beta$ . Note that here  $\varepsilon^{1/2}$  is a function of  $r$  equal to  $\varepsilon_w^{1/2} e^{S^2(r^2-1)/2}$ , where  $\varepsilon_w$  is the wall Ekman number that must be small in the whole flow. Generally, at high speed, the local Ekman number  $\varepsilon$  becomes of order the unity, or greater: in the core when  $r \lesssim 0.9$  then, the flow is diffusive and no complete solution has been given in this case. Fortunately, this region is of academic interest as the contribution of the axial mass velocity to the separative power is negligible. As the solution of the Ekman layer is very classical /1,2,10,13,.../ , it will not be mentioned here.

On the side wall ( $r=1$ ), the existence of two layers one of thickness  $O(\varepsilon_w^{1/3})$  merged into another one of thickness  $O(\varepsilon_w^{1/4})$  have been proved by Stewartson /20/. When the rate of injection or sampling located at radius  $r_1$  is of order  $O[\varepsilon^{1/6}(r_1)]$  the existence of a detached shear layer parallel to the axis of the cylinder has been shown experimentally and theoretically /21/. These 1/3 layers allow the passage of the flow rate from one plate to the other one. The Stewartson 1/4 layer ensures the transition of the azimuthal velocity from the core to the wall; this layer disappears in the case of an antisymmetric problem, using Stewartson's terminology /20/ :

$$v(z, r) = -v(-z, r), \quad \psi(r, z) = \psi(-z, r), \quad \bar{T}(r, z) = -\bar{T}(-z, r)$$

$\psi$  is the streamfunction. This is the case when the wall temperature is antisymmetric relative to the midplane  $z = 0$ . The expansion read, in the Stewartson 1/3 layer located at radius  $r_1$ ,

$$g(r, z, \varepsilon) = \tilde{g}(\xi, z, \varepsilon) = \tilde{g}^{(0)}(\xi, z) + \varepsilon_1^{1/2} \tilde{g}^{(1)}(\xi, z) + \varepsilon_1^{1/6} \tilde{g}^{(2)}(\xi, z) + \dots \quad (16)$$

where  $\xi = \frac{r - r_1}{\varepsilon_1^{1/3}}$ ,  $\varepsilon_1 = \varepsilon(r_1)$

and, in the Stewartson 1/4 layer  $\eta = (r - r_1) / \varepsilon_1^{1/4}$

$$g(r, z, \varepsilon) = \hat{g}(\eta, z, \varepsilon) = \hat{g}^{(0)}(\eta, z, \varepsilon) + \varepsilon_1^{1/2} \hat{g}^{(1)}(\eta, z) + \varepsilon_1^{1/6} \hat{g}^{(2)}(\eta, z) + \dots \quad (17)$$

The corners of size  $O(\varepsilon_1^{1/4})$ ,  $O(\varepsilon_1^{1/6})$ , called the Ekman extensions are singular: there, the quasi-complete systems are to be solved.

The approximation will be accurate if the first term of each expansion (14,15,16,17) is preponderant. It turns out that the local Ekman number must be smaller than  $10^{-2}$  and the wall Ekman number has to be smaller than  $10^{-6}$  to be neglected. In the centrifuge, all terms of the expansions must be computed up to the order  $\varepsilon^{1/2}$  which is the order of the countercurrent mass flow rate.

One can notice that the convergence of the expansions (14,15,16,17) is not ensured but that the first terms constitute a very good approximation.

The main features of our method are recalled here ; the details can be found in A3,14 / .

### 3.2. - Solution in the Stewartson 1/3 layer by axial eigenfunction

The Stewartson 1/3 layer has been calculated by assuming that  $\varepsilon_1^{1/3}$  is of order of magnitude the Mach number, so that

$$\varepsilon^* = 2\kappa_1 \varepsilon^{1/3} S^2 = O(1)$$

The resulting sixth order partial differential equation giving the stream function reads for the leading term

$$\frac{\partial^2 \tilde{\psi}^{(0)}}{\partial z^2} + P \tilde{\psi}^{(0)} = 0 \quad (18)$$

with the boundary conditions

$$\tilde{\psi}^{(0)} = \frac{\partial \tilde{\psi}^{(0)}}{\partial \xi} = 0 \quad \xi = 0 \quad (\text{side-wall})$$

$\tilde{\psi}^{(0)}$  and its derivatives bounded as  $\xi \rightarrow -\infty$  (matching conditions with inviscid core)

$$\tilde{\psi}^{(0)} = 0 \quad z = \pm \beta \quad (\text{matching with extensions})$$

where  $\xi = \frac{z-1}{\varepsilon_1^{1/3}}$  is the inner variable and

$$\mu^{(0)} = \frac{\partial \tilde{\psi}^{(0)}}{\partial z}, \quad w^{(0)} = -L \tilde{\psi}^{(0)} \quad (19)$$

$$P = \varepsilon^{-2} - 2\varepsilon^* \xi (D-1)^2 D^2 (D+1) \quad (20)$$

$$D = \frac{\partial}{\partial \xi}$$

The solution is found in terms of Fourier series ; for example in the case of an antisymmetric problem.

$$\tilde{\psi}^{(0)} = \sum_{n=1}^{\infty} f_n(\xi) \cos\left(\frac{n\pi z}{2\beta}\right) \quad (21)$$

This term gives rise to a close recirculation flow of the order  $\epsilon^{1/3}$  in the Stewartson 1/3 layers. The non vanishing next order

$$\tilde{\psi}^{(2)} = E(\xi) + \sum_{n=1}^{\infty} g_n(\xi) \cos\left(\frac{n\pi z}{\beta}\right) \quad (22)$$

corresponds to the countercurrent mass flow rate of the order  $\epsilon^{1/2}$  driven by the Ekman suction condition,  $E(\xi)$  is given by the Ekman extensions /13/ .

### Remarks

1. Note here that this method can be regarded as an eigenfunction method in  $z$  as the conditions are homogeneous at the first order  $\tilde{\psi}^{(0)}$  and the next order  $\tilde{\psi}^{(2)}$  (passage of the mass flow rate) is rendered homogeneous easily by a change of dependant variables.

2. The Fourier method is usually slowly convergent so that Padé approximants /22/ have been used to reduce computing time and improve accuracy especially for detached shear layers. Then, seven terms are used and the relative accuracy is about  $10^{-3}$ . On the contrary, without convergence acceleration, about thirty terms are needed and the relative is only about 3 %. When  $\epsilon^*$  increases, the accuracy and the rate of convergence of the computation decrease.

Typical values of the computing times on CDC 7600 are 30s for one detached layer with convergence acceleration and 10s for a wall layer. Notice that the program computing the analytical method uses a great number of points in  $r$  and  $51 \times 11$  to  $101 \times 11$  in the Stewartson 1/3 layer and that the execution time has not been specially optimized.

One advantage of the method is that the computation is done for a given value of the parameter  $\epsilon^* = 0.1$ . Thus the use of similarity criteria yields the computation of a family of layers linked by a relation with various  $n, \epsilon, S^2$  and fixed  $\beta$ . As  $\epsilon$  varies, the summation of the Fourier series has only to be performed again and is very short ( $\sim 1s$ ).

The solution found here is the sum of the development in  $\epsilon^*$  in NAKAYAMA's solution /21/ with the same boundary conditions. But in /21/ only the first correction due to the compressibility effect was computed.

#### 4. - RADIAL EIGENVALUE METHOD

4.1. - After the preliminary work from STEENBECK /4/, in which the temperature was not taken into account, PARKER and MAYO /5/ carried out the following eigenvalue method:

- Separation of variables is assumed of the form

$$\psi(r, z) = f(r) g(z) \quad (22.a)$$

- The boundary layers on the end-cap (Ekman layer or extensions) were excluded as the viscous terms become preponderant and are useful to compute this complete flow.

- The region from  $0 \leq r \leq 1$  is treated as completely viscous. No split between inviscid, viscous, boundary layer at the side wall is made.

The solution is obtained at  $r = 0$  with axis conditions :

$$u = v = 0, \quad \frac{\partial T}{\partial r} = \frac{\partial \psi}{\partial r} = 0 \quad (23)$$

and on the wall with the following conditions,

$$u = v = w = 0, \quad T = 0 \quad (\text{or } \frac{\partial T}{\partial r} = 0) \quad (24)$$

Unfortunately, the resulting differential linear system of equations with two-point boundary conditions, is very difficult to solve at high values of  $S^2$  because of exponential increasing values and "parallel solutions" so that the determinant to solve becomes pure noise. For the value of  $S^2 = 25$ , PARKER and MAYO /5/ found only one eigenvalue and one eigenfunction so that it was impossible to expand the end caps solutions on an orthogonal basis of functions. Furthermore, no proof of the orthogonality nor weight functions were given as the operator of /5/ was not simple..

JACQUES /23/ has derived a solution for a low radial decay so that average velocities are taken in the axial direction, by integrating the equations axially. By coupling with the Ekman layers and determining thus the unknown constants, the absolute amount of the flow can be computed. Unfortunately, this solution is insensitive to the temperature distribution of the side walls, due to the small order (4th) of the final differential system to be solved.

4.2. - Asymptotic method

Then, asymptotic methods were used assuming  $S^2 \gg 1$  by GING /7/ and BROUWERS /8/ whose results are equivalent in the limit  $S^2 \rightarrow \infty$ . Hence we will try here to give a complete solution using BROUWERS's method. It consists in setting

$$\alpha = 2S^2(x-1) \quad (25)$$

as a variable, in fact an inner variable.

Then, the layer has a thickness  $1/S^2$  which is of the same order as a classical Stewartson 1/3 layer if  $(\beta \epsilon)^{1/3} S^2 = O(1)$  and one can notice that also the thermal quantity  $y = rT - 2v = O(1)$  present the usual scaling of the Stewartson 1/3 layer. With this scaling, the system reduces after some algebra to :

$$\frac{\partial \gamma}{\partial z} = \alpha^2 A \hat{\psi} \quad (26)$$

$$\frac{\partial \hat{\psi}}{\partial z} = -B \gamma \quad (27)$$

with

$$A = \frac{\partial}{\partial x} e^{-\alpha} \frac{\partial^2}{\partial x^2} \left( \frac{\partial^2}{\partial x^2} + 1 \right) \quad (28)$$

$$B = - \frac{S^4 \epsilon \beta e^{-\alpha}}{1+h} \frac{\partial^2}{\partial x^2} \quad (29)$$

$$\psi = 2\epsilon\beta S^4 \hat{\psi} \quad (30)$$

$$\alpha^2 = \frac{64\epsilon^2 \beta^2 S^{12}}{1+h} \quad (31)$$

In fact, an equivalent system has been studied by LOUVET-DURIVAUULT /13/ and by BROUWERS /8/; it will be solved for fixed  $\alpha$  which means that  $S^2 = O(\epsilon\beta^{-1/3})$ .

BROUWERS /8/ assumed that this system is valid in a wide region, at least in the long cylinder case, since it matches with a proper Ekman layer, not at extension near the end caps. The core is assumed to be matched straightly with a viscous zone :  $\frac{\partial \psi}{\partial x} = \frac{\partial \gamma}{\partial x} = 0$ . This is surely true for long centrifuges.

Here, we will investigate the matching with an extension and with an Ekman layer. The system (26,27) can be solved in  $\hat{\psi}$  and leads to the eq. (18) written in a new form.

$$\frac{\partial^2 \hat{\psi}}{\partial z^2} - BA \hat{\psi} = 0 \quad (32)$$

where  $BA = P$  (to a multiplicative constant) which has to be solved with the following boundary conditions

$$z = \pm \beta, \text{ matching with Ekman layers or extensions,}$$

$x \rightarrow -\infty$ , applying the matching conditions with the core given in /24/ and assuming only  $\gamma = O(1)$ ,  $w = O(1)$ ,  $x$  bounded away from zero, we find

$$\frac{\partial \gamma}{\partial x} = \frac{\partial w}{\partial x} = \frac{\partial^2 w}{\partial x^2} = 0 \quad (33)$$

In terms of  $\hat{\psi}$ , the last two conditions read

$$\frac{\partial}{\partial x} \left( \frac{\partial}{\partial x} + 1 \right) \hat{\psi} = \frac{\partial^2}{\partial x^2} \left( \frac{\partial}{\partial x} + 1 \right) \hat{\psi} = 0 \quad (34)$$

$x=0$  (wall),  $u=v=w=0$ ,  $T = T_w(z)$ , conditions which are equivalent to

$$\hat{\psi} = \frac{\partial \hat{\psi}}{\partial x} = \psi^{(IV)} - \frac{\partial^2 \psi}{\partial x^2} = 0 \quad (35)$$

Now, to obtain an eigenvalue problem, one must deduce the inhomogeneous part of the boundary conditions at  $x=0$  by setting

$$\hat{\psi} = -\varphi(x) F'(z) + \sum_{k=0}^{\infty} \frac{g_k(z) f_k(x)}{\psi_1} \quad (36)$$

where  $F'(z) = T_w'(z)$  and  $\varphi(x) = \frac{1}{2} [1 + e^x(x-1)]$

The eigenfunctions  $f_k(x)$  are solutions of the eigenvalue problem

$$BA f_k + \lambda_k f_k = 0 \quad (37)$$

with the homogeneous conditions (34) and (35).

Eq.(34) are equivalent to those of BROUWERS /8/ with respect to eq.(37)

Putting (36) into (32), the system reduces to solve

$$\frac{\partial^2 \hat{\psi}_i}{\partial z^2} - BA \hat{\psi}_i = \varphi(x) \frac{d^3 T_w(z)}{dz^3} \quad (38)$$

The eigenproblem for the thermal wind quantity  $\gamma_k$  is the adjoint problem so that

$$\int_0^{-\infty} e^x \gamma_k f_j dz = 0 \quad \text{for } k \neq j \quad (39)$$

Then, multiplying the two terms of eq. (38) by  $e^x \gamma_k$ , we obtain for  $g_k$

$$\frac{d^2 g_k}{dz^2} - \alpha^2 \lambda_k g_k = \varphi(x) \frac{d^3 T_w}{dz^3} \quad (40)$$

whose solution is given by ( $\lambda k < 0$ )

$$g_k(z) = \alpha_k e^{-\alpha \sqrt{-\lambda k} z} + \beta_k e^{\alpha \sqrt{-\lambda k} z} + g_{pk} \quad (41)$$

and  $g_{pk}$  is a particular solution of the linear differential equation. In the case of a linear side wall temperature profile this particular solution vanishes.

Remark : The eigenvalue  $\lambda_{k=0}$  gives rise to a solution in the form  $\psi = A + Bz$  which can be considered either as a long bowl solution or as a Stewartson 1/4 layer solution for short bowl since, if  $S^2 = O(\epsilon^{-1/4})$

$$\alpha^2 = 0 + O(\epsilon^{1/4})$$

The solutions of (37) satisfying (34) are of the form

$$f_k(x) = \sum_{n=0}^{\infty} (a_n k e^{2nx} + b_n k e^{(2n+1)x} + c_n k e^{(2n+1)x}) \quad (42)$$

Omitting the dependance with respect to  $k$  and setting:

$$\begin{aligned} a_n &= \lambda^n A_n a_0 \\ c_n &= \lambda^n C_n c_0 \end{aligned} \quad (43)$$

$$b_n = \lambda^n C_n (b_0 + c_0 \sigma_n) = \beta_n C_n$$

and replacing in the equation (37), this leads by identification to

$$A_n = \frac{A_{n-1}}{P_n} = \frac{A_{n-1}}{(2n-1)^2 4n^2 (2n+1)} \quad (44)$$

$$C_n = \frac{C_{n-1}}{16n^3 (2n+1)^2 (n+2)}$$

$$\beta_n = \lambda \beta_{n-1} - \sigma_n = \lambda \beta_{n-1} - \sum \frac{P'(\xi_{n+1})}{P(\xi_{n+1})}$$

Thus the set of functions satisfying (34) and (37) reads

$$a_0 \sum_{n=0}^{\infty} \lambda^n A_n e^{2nx} + b_0 \sum_{n=0}^{\infty} \lambda^n C_n e^{(2n+1)x} + c_0 \sum_{n=0}^{\infty} \lambda^n [C_n (x + \sigma_n)] e^{(2n+1)x} \quad (45)$$

For given  $\lambda$ , the conditions (35) give rise to a linear homogeneous system of three equations for  $a_0, b_0, c_0$ , and the equation for the eigenvalues expresses that the determinant of the system is zero. This last equation reads as

$$\sum_{\ell=0}^{\infty} \alpha_{\ell} = 0 \quad (46)$$

$$\text{with } \alpha_{\ell} = \sum_{m+n+p=\ell} D_{mnp} \quad (47)$$

and  $D_{mnp}$  is a third order determinant which can be written as

$$\begin{aligned} D_{mnp} &= A_m A_n C_p \sigma_p (N-M)(P-M)(P-N) (P^{\ell} + M^{\ell} + N^{\ell} + NP + PM + MP - i) \\ &\quad + A_m A_n C_p [\ell P (\ell P^{\ell} - 1) - (M+N)(M^{\ell} + N^{\ell} - 1)] \end{aligned} \quad (48)$$

where  $M = 2m$ ,  $N = 2n + 1$ ,  $P = 2p + 1$

The resolution is achieved by Newton's method, using to compute the roots of the polynomial of degree  $l + 1$ , the already found  $l - 1$  roots of the polynomial of degree  $l$ ; the last root uses as starting point a trial value so that  $\lambda_l \approx \epsilon$  to  $5 \lambda_{l-1}$ . The value of the polynomial is computed by HORNER's algorithm. The constant  $c_0$  is arbitrarily set to 1, as the determinant (3 x 3) of the full linear system is assumed to vanish for the eigenvalues  $\lambda_l$ . The last constants  $a_0, b_0$  are solutions of

$$\left( \sum_{n=1}^k \lambda_l^n A_n \right) a_0 + \left( \sum_{n=1}^k \lambda_l^n C_n \right) b_0 + \left( \sum_{n=1}^k \lambda_l^n C_n \sigma_n \right) \cdot 1 = 0$$

$$\left( \sum_{n=1}^k 2n \lambda_l^n A_n \right) a_0 + \left( \sum_{n=1}^k (2n+1) \lambda_l^n C_n \right) b_0 + \sum_{n=1}^k \lambda_l^n C_n (1 + \sigma_n (2n+1)) = 0$$

so that the three boundary conditions are fulfilled for the eigenvalue  $\lambda_k$ . In the table 1, the computed eigenvalues are given.

The number of terms in the summation is chosen so that the ratio of two consecutive terms of the sequence is small enough; thus, the series in (42) have already converged up to the rounding errors. Then, the eigenfunctions  $f_k$  and their adjoint  $Y_k$  are computed by

$$f_k = \sum_{n=1}^L [a_n e^{2nx} + b_n e^{(2n+1)x} + c_n x e^{(2n+1)x}] \quad (50)$$

$$Y_k = \sum_{n=1}^L [a_n 4n^2 (4n^2 - 1) e^{2nx}] + \sum_{n=1}^L \{ b_n (2n+1)^2 e^{2nx} + c_n ((2n+1)^2 - 1) x e^{2nx} \} \cdot [(2n+1)^2 - 1]$$

$$+ \sum_{n=1}^L \{ 2c_n (2n+1) [2(2n+1)^2 - 1] e^{2nx} \} \quad (51)$$

The results are shown on the figure 2, after having set the asymptote to 1 by rescaling. Note that  $\varphi$  is very close to  $\psi_1$  and that the zeros of the eigenfunctions are intricated. Notice that as  $k$  increases,  $|\lambda_k|$  does and the series giving  $f_k$  and  $Y_k$  get more and more difficult to compute due to a decrease of convergence rate.

LAMDA= -5.812807	I= 1	LAMDA= -90534.47	I= 6
LAMDA= -228.0873	I= 2	LAMDA= -215811.4	I= 7
LAMDA= -1968.678	I= 3	LAMDA= -464561.8	I= 8
LAMDA= -9438.013	I= 4	LAMDA= -929466.8	I= 9
LAMDA= -32529.36	I= 5	LAMDA= -1519250.	I= 10

Table I - Eigenvalues of eq. (37)

## 5. - CENTAURE CODE

This code uses finite element method which allows to refine the mesh in the boundary layers and to divide radially the cells into equal mass rather than equal distance.

This is a main advantage on the finite difference method to investigate accurately the boundary layers. The elements are quadrilateral and the discretization is bilinear with respect to local coordinates. The resulting linear system is solved by GAUSSIAN elimination using blocks. The solution is assumed to be obtained when the refining of the mesh does not change the solution. In most of the cases, a mesh 20 x 31 is sufficient (fig.4). The first iteration (linear run) is compared with the other methods. The cost varies as  $n_x \sqrt[3]{n_z}$  where  $n_x$  and  $n_z$  are the dimensions of the mesh. With a 20 x 31 mesh and an IBM 360/S91 computer, typical cost /19/ are given in table 2.

Execution type	Region (bytes)	CPU time	Number of input/outputs
Operator calculus	500 K*	18 min	3000
First linear run (5 equations)	600 K*	6 min	3500
Further linear runs (5 equations)	600 K*	45 sec	3000
Nonlinear run (5 equations, $n$ Newton iterations)	600 K*	$n \times 6$ min	$2500 + n \times 1000$

TABLE II- Computing cost /19/

## 6. - COMPARISON BETWEEN THE THREE METHODS

### 6.1. - Comparison cases

The CENTAURE Code was checked initially /19/ with an antisymmetric case of pure thermal countercurrent at low speed ratio  $S^2 \sim 10$  /26/ for which almost no doubt could rise as the compressibility effect was very small. The data read

Height of the cylinder $H$	60.6 cm
Radius of the cylinder $R$	7.35 cm
Peripheral rotation speed $\omega R$	400 m/sec
Process gas $UF_6$	
Gas pressure at the periphery	$1.33 \times 10^4$ Pascal
Temperature of the bulk of the gas $T_0$	308 K

Deviation of temperature in end caps generating the countercurrent $\Delta T/T_0$	0.033
Side wall perfectly conducting at a temperature increasing linearly in $z$ from $T_0 - \delta T$ at $z = 0$ to $T + \delta T$ at $z = H$	
Viscosity of the gas	$200 \times 10^{-6}$ poise
Molecular mass $M$	352 g
Specific heat ratio $\gamma$	1.065
Prandtl number $Pr$	0.75
Isotopic mass difference $\Delta M$	3 g
Schmidt number $Sc = \mu/\rho D$	0.75

The two results were found to agree better than 1%.  
In this work, three other cases will be investigated.

CASE A : A pure thermal antisymmetric countercurrent case with

$$\left. \begin{array}{l} S^2 = 25 \\ \epsilon_w = 3.26 \cdot 10^{-8} \\ \beta = 5 \end{array} \right\} 2 \epsilon_w^{1/3} S^2 \approx 0.16$$

The countercurrent is generated by heating the plate  $z = \beta$  at a constant  $T_0 + \Delta T$  and cooling the plate  $z = -\beta$  at  $T_0 - \Delta T$ , while the profile along the side wall is taken linear between this two values.

CASE B : A case showing the profile of inner detached layer

$$\left. \begin{array}{l} S^2 = 32 \\ r_1 = 0.912 \\ \beta = 1.57 \\ \epsilon_w = 1.97 \cdot 10^{-8} \\ \epsilon_A = 4.37 \cdot 10^{-6} \end{array} \right\} 2 \epsilon_A^{1/3} \pi_1 S^2 \approx 0.95$$

The code uses a discretized parabole using four meshes between 0.903 and 0.916. All the input mass flow was assumed to exit at the same radius. The location of the injection for the matched asymptotic method was supposed to be the mean radius of the input mass velocity profile.

CASE C : A symmetric case C with

$$S^2 = 1$$

$$\varepsilon_w = 2 \cdot 10^{-7}$$

$$\beta = 2$$

$$T = T_0 \text{ on the two end caps } z = \pm \beta \text{ and } T = T_0 + \Delta T \left(1 + \cos \frac{\pi z}{\beta}\right) \text{ on the lateral side wall.}$$

The other data for the computation read

$$\gamma = 1.065, \text{ Pr} = 0.96, \text{ M} = 0.352, T_0 \approx 310 \text{ K}$$

Deliberately, the CENTAURE Code results are generally not smoothed on the various figures so that one can see the mesh points and we do not use a composite expansion in the matching regions so that the different layers can be seen.

## 6.2. - CASE A

The result of the CENTAURE Code is compared on figures 6 to 12 with the results obtained by LOUVET and DURIVAUULT /13, 15/ for the axial, radial and azimuthal velocity. For the axial velocity, the agreement is better than 3 % in the Stewartson layer (fig. 6 , 7 ) but two terms corresponding to the closed recirculation (mass flow rate of the order  $\varepsilon_w^{1/2}$ ) and to the passage of the mass flow rate or countercurrent flow (mass flow rate of the order  $\varepsilon_w^{1/2}$ ) are needed. One term  $\tilde{w}^{(0)}$  will give an agreement of only 10 % (fig.5). Using incompressible approximation  $\rho = \text{ct}$  in the Stewartson layer would have been worse. For the radial velocity  $\tilde{u}^{(0)}$  (fig.8) which is  $\varepsilon_w^{1/3}$  smaller than  $\tilde{w}^{(0)}$  as the scale analysis yields in the Stewartson 1/3 layer, the CENTAURE Code gives an irregular profile probably due to relative errors in the final Gaussian elimination as  $u$  is too small. The same result occurs in the Ekman layers for the less dominant velocity which is now  $w$  (fig.11,12). For the azimuthal velocity (fig.9) some discrepancies due probably to the slow convergence of the Fourier series arise. This is confirmed by the fact that the "incompressible" solution gives a better result and that no convergence acceleration has been used here.

On the fig.10, as far as  $\varepsilon_w^{1/2} S^2 \ll 1$ , the radial and azimuthal velocity of order the unity obtained by the two methods are in correct agreement.

Notice that if  $\epsilon^{1/2} S^2 = O(1)$ , the axial mass velocity which occurs for the calculation of the separation is already negligible.

On the other hand, the mesh refinement is more crude when  $r$  decreased so that non smoothed curves are less accurate. CENTAURE Code results gives approximately a region of inviscid flow between  $0.8 \leq \kappa \leq 0.95$ . For  $\kappa \leq 0.8$ , as the Ekman number becomes not small and as the aspect ratio is of order the unity, the hypothesis derived in /15/ becomes invalid in the diffusive region.

Thus, the presence of Stewartson 1/3 layer, of an inviscid core and a diffusive region turns out clearly.

### 6.3. - CASE B

The adequacy between the two methods is less good (Fig.13) but some important remarks turn out .

- a) The detached layer is very thick in the middle plane ; as the density decreases exponentially with  $\kappa$ , important corrections of curvature must be done like those proposed by BARK /12/ . The correction of curvature in matched asymptotic method should increase the velocity in the center and push more the gas towards the wall  $\kappa = 1$ . This phenomena is qualitatively already a result of the CODE and of the first order of our method.
- b) The methods are sensitive to the location of the injection : for exemple if one replaces the injection located at the mean axial mass velocity ( $\kappa = 0.912$ ) by an injection located at the mean axial velocity ( $\kappa = 0.9095$ ) : modifications up 10% in certain regions are obtained !  
One can expect that the shape of the profile is also important.
- c) The method of asymptotic expansions with the numerical solution in /13/ gives rise to convergence trouble especially for the azimuthal and radial velocity due to the derivation in the Fourier series.
- d) In fact the CENTAURE Code, treated a case with an inner cylinder and showed the appearance of a wall layer which can be due to the non-damping of the detached layer : notice that a 1% residue, even numerical, can be important in terms of axial mass velocity as the density increases very quickly. This layer can be also due to the circumferential curvature effect. This point seems to be open.

6.4. - CASE C

This case is a symmetric case at small speed ratio  $S^2 = 1$  in order to investigate the influence of the boundary conditions and of discontinuities in the corners  $\gamma = \pm\beta$ ,  $\lambda = 1/26$ . The Ekman number is  $2 \cdot 10^{-7}$  and  $\beta = 2$ . In fact, this case was run in two times one with

$T = T_0$  on the end caps

$T = T_0 + \Delta T$  on the side wall

one with

$T = T_0$  on the end caps

$T = T_0 + \Delta T \cos\left(\frac{n\pi z}{\beta}\right)$

The sum of the two cases has been drawn on the fig 14. and 15. As only the leading term has been derived for the computations the agreement is satisfactory for the axial and azimuthal velocity. The same problems arise for the radial velocity profile as in the antisymmetric case due most probably to the CENTAURE Code. With the prescribed boundary conditions, the leading terms in the asymptotic expansions in the core and the Ekman layers vanishes so that the flow outside the Stewartson layers is negligible. This fact is confirmed by the results of the CENTAURE Code in the core.

6.5. - EIGENVALUE METHOD

This method works fairly for  $\alpha$  of unit order, which is in particular the case of long centrifuges. Unfortunately, in the method described in 4.2., numerical difficulties arise for small  $\alpha$ , due to a decrease of convergence rate. In the cases computed here  $\alpha$  is of order  $10^{-2}$ .

For this reason, no comparison with A,B,C has been performed in the present work.

## 7. - CONCLUSIONS

For the different cases studied here : symmetric, asymmetric and detached layers, the numerical solution of the linearized system computed with CENTAURE Code and the solution found by LOUVET and DURIVAUT /13/ agree satisfactorily.

The "so called" eigenvalue method seems more adequate for long machines. As the system to solve at high speeds of rotations is the same as in /13/ near the side-wall, the boundary layer and eigenfunctions methods differs only by the use of radial eigenfunctions instead of axial ones.

-----

REFERENCES

- /1/ GREENSPAN, HP  
Theory of rotating fluids - 1968 - Cambridge University Press.
- /2/ SOUBBARAMAYER  
Centrifugation chap. 4 - to be published by Vilani in Springer-Verlag Series - 1979.
- /3/ RATZ  
Centrifugation - Course on isotope separation at the Institute Von Karman, (1978).
- /4/ STEENBECK M.  
Erzeugung einer selbstkaskadierenden Axialströmung in einer langen Ultrazentrifuge zur Isotopentrennung - Kernenergie 1. Jahrgang Heft 11/58 .
- /5/ PARKER H.M. and MAYO T.T.  
Countercurrent flow in a semi-infinite Gas Centrifuge preliminary results. Report N° E.P. - 4422 -279-63 U Jan. 1963  
Research Laboratories for the Engineering Sciences  
University of Virginia, Charlottesville Virginia.
- /6/ SOUBBARAMAYER  
Solutions approchées du contre courant thermique dans les centrifugeuses  
Rapport CEA-R-4186 - 1971.
- /7/ GING J.  
Countercurrent flow in a semi-infinite gas centrifuge. Axially symmetric solution in the limit of high angular speeds.  
Report N° EP 4422 -198-62 U Jan. 1962 .
- /8/ BROUWERS J.J.H.  
On the motion of a compressible fluid in a rotating cylinder  
PH. D. Thesis, Twente Institute of Technology, Enschede,  
The Netherlands, June 1976.
- /9/ MATSUDA T., SAKURAI T., and TAKEDA H.  
Source-sink flow in a gas centrifuge  
J. Fluid Mechanics - 1975, 69, 197-208.
- /10/ SAKURAI T., and MATSUDA T.  
Gas dynamics of a centrifugal machine  
J. Fluid Mechanics - 1974, 62, 727-736.
- /11/ BARK E.H. and BARK T.H.  
On vertical boundary layers in a rapidly rotating gas  
The Royal Institute of Technology Sweden  
Department of Mechanics  
TRITA-MEK- 76 - 07.

- /12/ BARK F.H. and MEIJER P.S.  
 Some properties of E<sup>4/3</sup> layers in rapidly rotating gases,  
 Proceeding of the Second Workshop on Gases in Strong Rotation  
 Cadarache - France - April 1977.
- /13/ LOUVET P. and DURIVALT J.  
 Compressible countercurrent flow in a strongly rotating cylinder,  
 Lecture Notes in Mathematics Springer-Verlag (1978) - vol. 594, p. 312-333.
- /14/ LOUVET P.  
 Two and three dimensional rotating flows,  
 Proceedings of the Second Workshop on Gases in Strong Rotation,  
 Cadarache, France, April 1977.
- /15/ DURIVALT J. and LOUVET P.  
 Etude de la couche de Stewartson compressible dans une centrifugeuse  
 à contre courant thermique,  
 CR. Acad.Sci. Seance du 10 mars 1976, Series B, t 283, 1979.
- /16/ LOPEZ S.  
 Numerical calculation by finite difference method into a centrifuge  
 in the presence of a baffle,  
 Presented at Euromech 80  
 Separation Phenomena in gas mixture flows  
 Strömungsmechanik und strömungsmaschinen  
 Heft 22, Juni 1977, Verlag G. Braun Karlsruhe.
- /17/ LOPEZ S.  
 Comparison between the flow in a mechanically driven centrifuge,  
 calculated by means of a numerical code using the finite difference method,  
 Proc. of Second Workshop of Gases in Strong Rotation,  
 Cadarache, France, April 1977.
- /18/ KAI T.  
 Basic characteristic of centrifuges (III)  
 Analysis of fluid flow in centrifuges  
 Journal of Nuclear Science and Technology  
 14 (4), pp. 267-281, April 1977 .
- /19/ LA HARGUE J.P. and SOUBBARAMAYER  
 A numerical model for the investigation of the flow and isotope  
 concentration field in a centrifuge,  
 Computers Methods in Appl. Mech. and Eng., 15, 2, 1978, p. 259-273.
- /20/ STEWARTSON K.  
 On a almost rigid rotations,  
 J. Fluid Mechanics, 1957, 8, 17-26 .
- /21/ NAKAYAMA W. and USUI S.  
 Flow in rotating cylinder of a gas centrifuge,  
 J. Nucl. Sci. Tech., 1974, 11, 242-262 .

/22/ BAKER G.A.

Essential of Padé approximants.  
Academic Press, New-York, 1975.

/23/ JACQUES R.

Etude théorique du contre courant dans une ultracentrifugeuse.  
Résolution approchée des équations du contre courant.  
Rapport CEA-R-4336, CEN-Saclay - 1971.

/24/ CORTET C. and LOUVET P.

Properties of boundary layers generated by mechanically and thermally driven flows in a centrifuge. Cf. present proceedings.

/25/ P.A.M. Dirac

The motion in a self-fractionating centrifuge,  
General Electric, General Engineering Labs, Schenectady NY,  
Report N° Br 42, 1940.

/26/ DURIVALT J. and LOUVET P.

Etude théorique de l'écoulement dans une centrifugeuse à contre-courant thermique, 1976,  
Rapport CEA-R-4714, Commissariat à l'Energie Atomique, France .

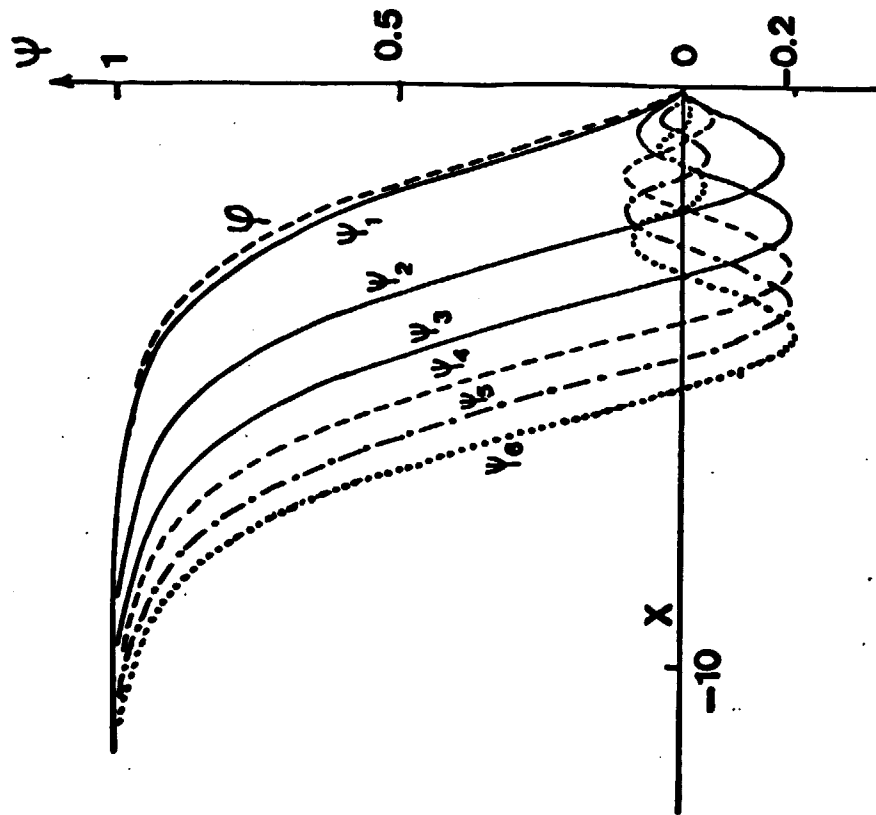


FIG 2 : Stream eigenfunctions profile  $\Gamma = 1.6$

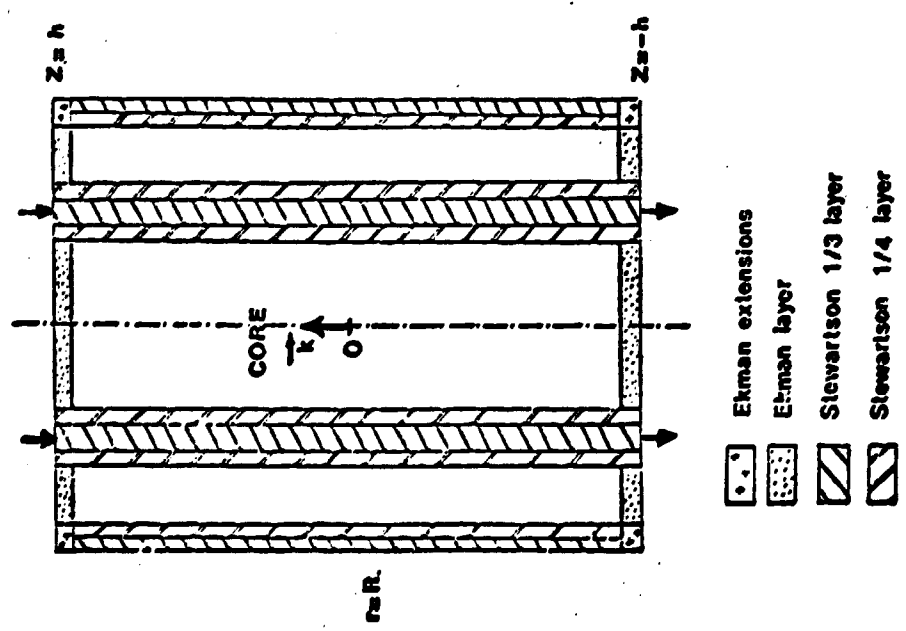


Fig. 1. Scheme of a centrifuge

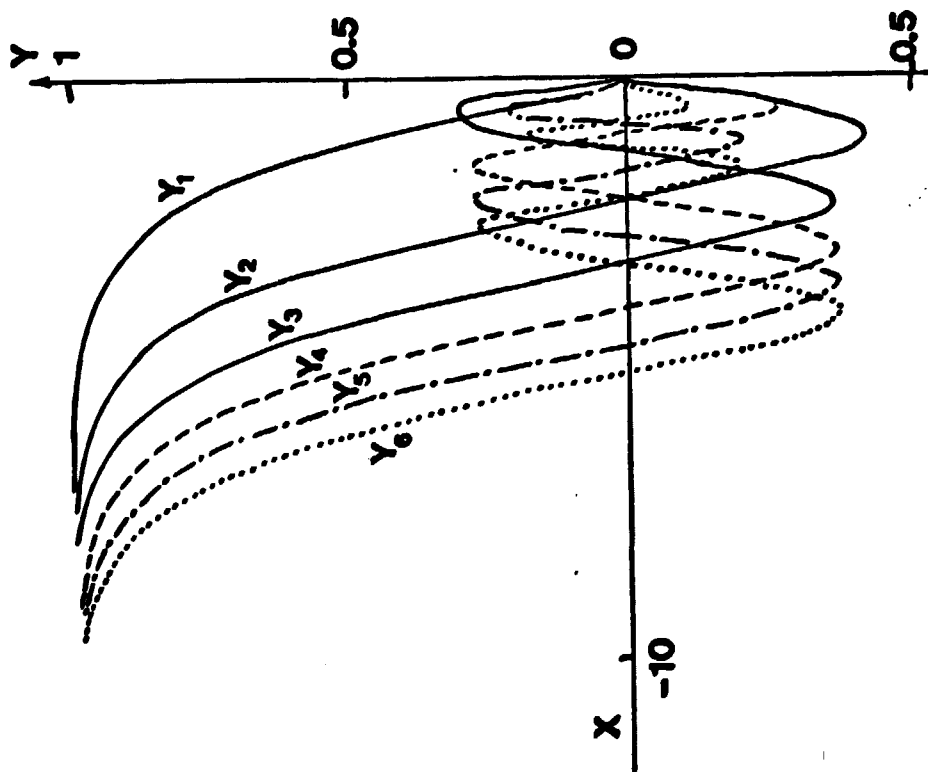


FIG 3 : Eigenfunctions of the adjoint operator  $\lambda = 1.6$

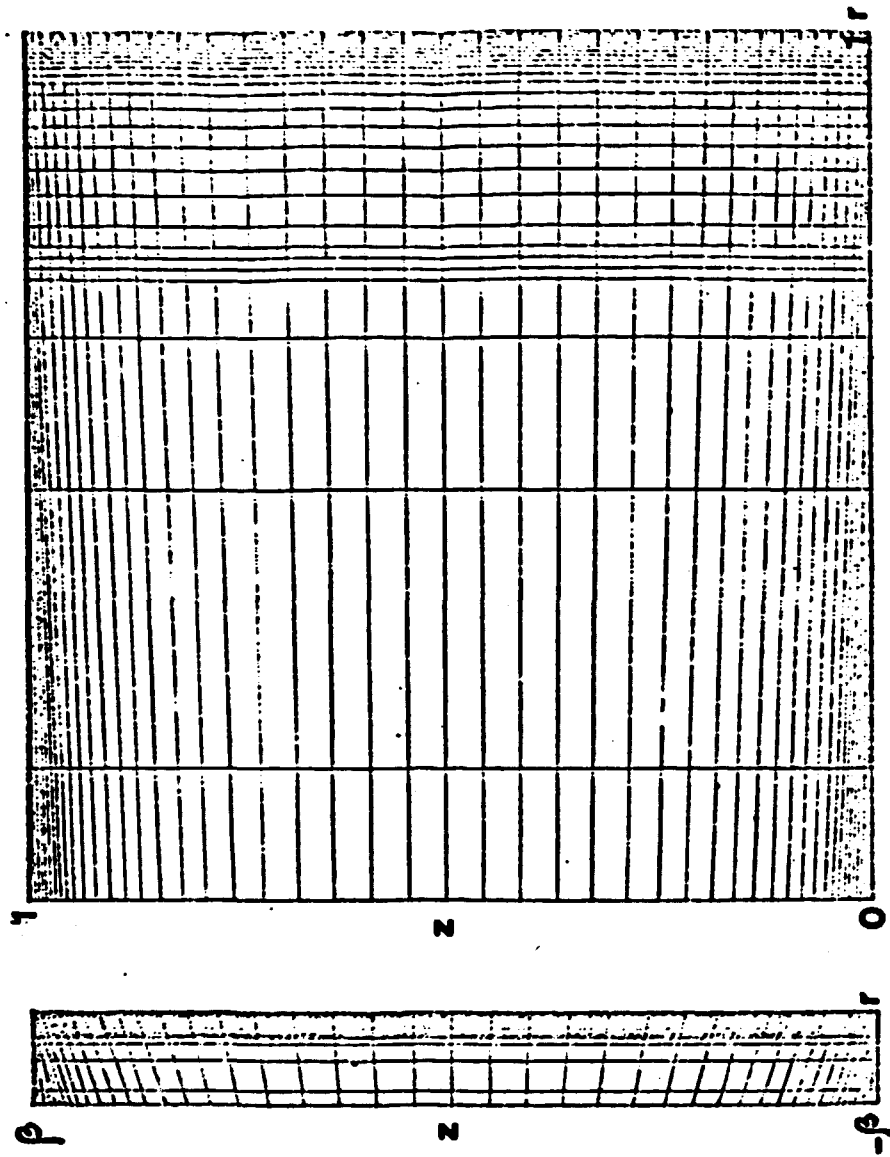
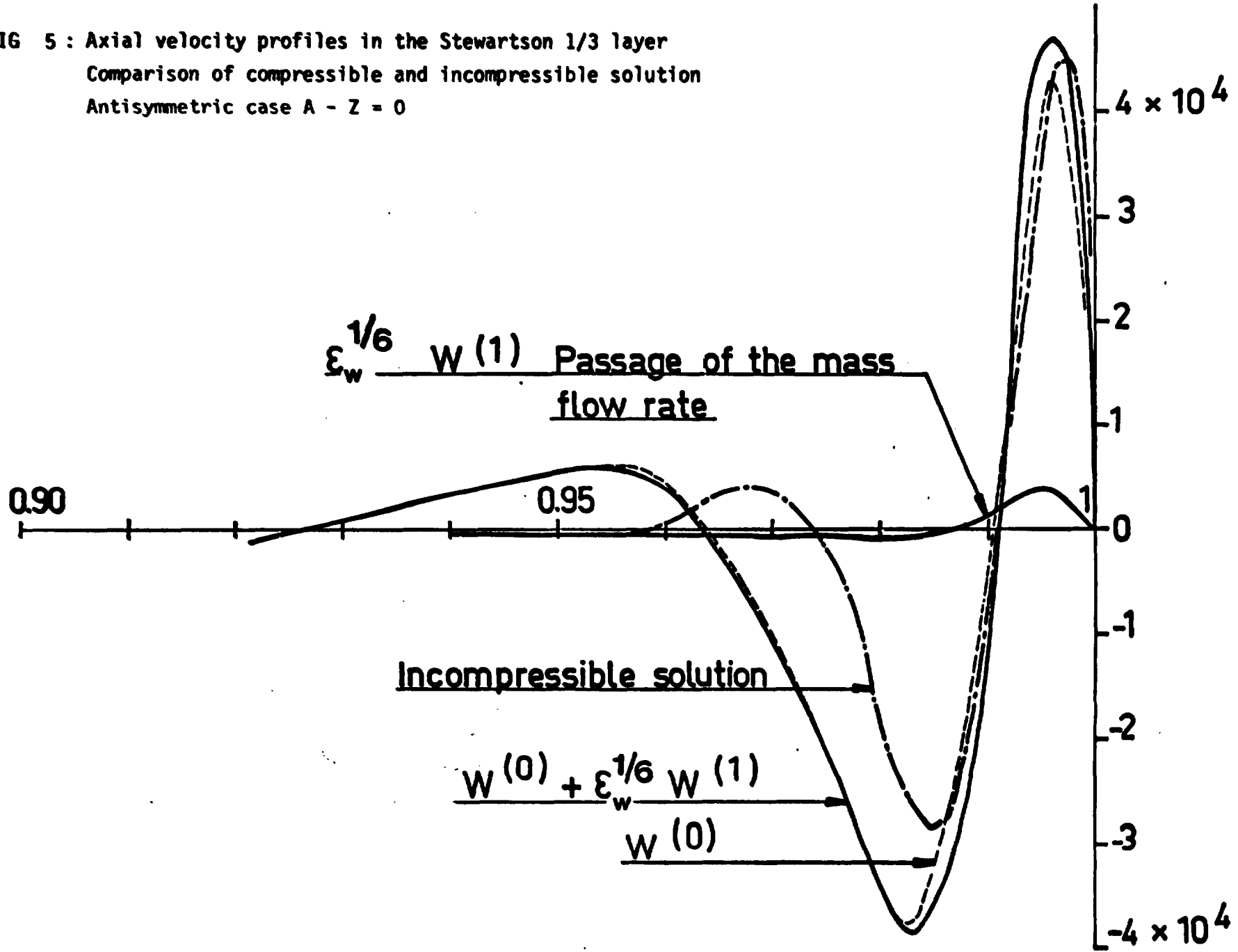


FIG 4 : Finite element meshes used in case B, for detached layers

FIG 5 : Axial velocity profiles in the Stewartson 1/3 layer  
 Comparison of compressible and incompressible solution  
 Antisymmetric case A - Z = 0



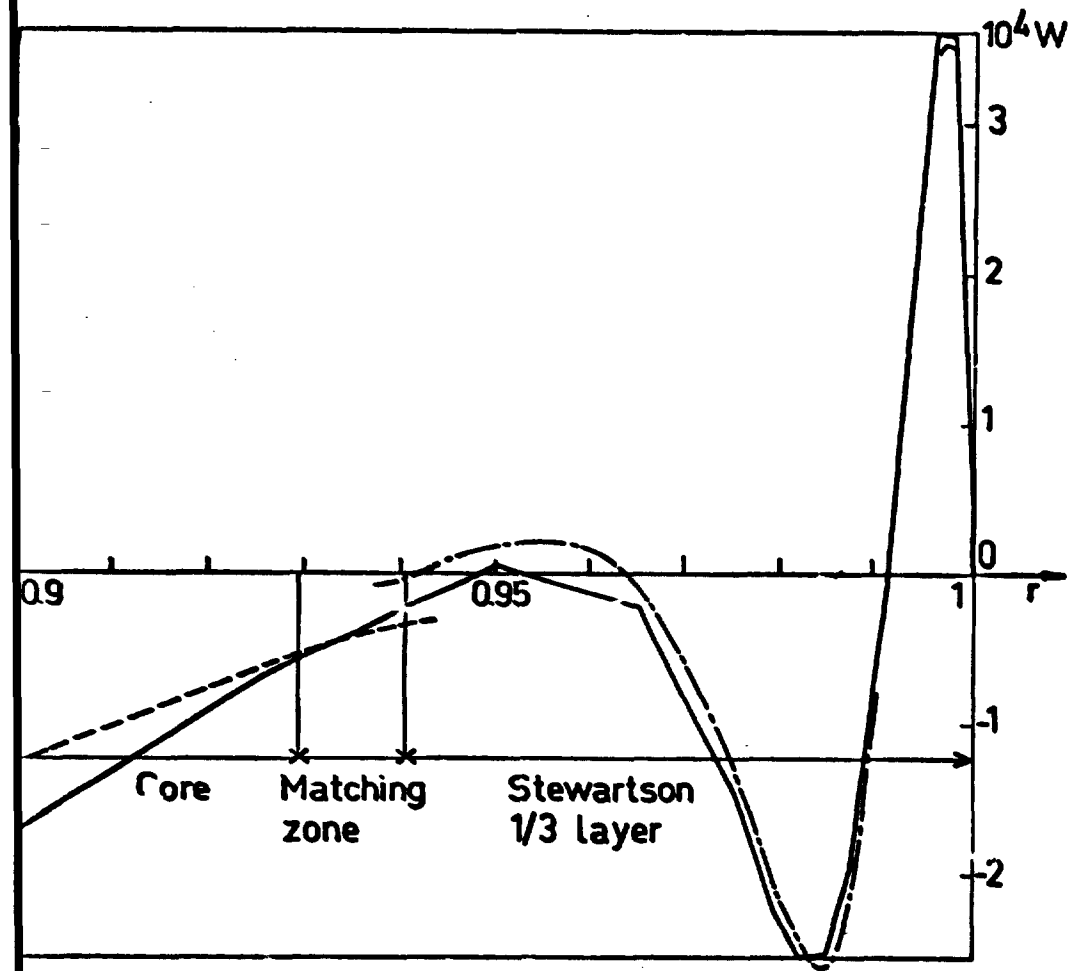


FIG 6 : Axial velocity profile near the wall in the mid plane,  $Z = 0$

Antisymmetric case A

— CENTAURE CODE

- - - Stewartson 1/3 layer : 2 terms  $w^{(0)} + \epsilon^{1/3} w^{(1)}$

--- Core solution

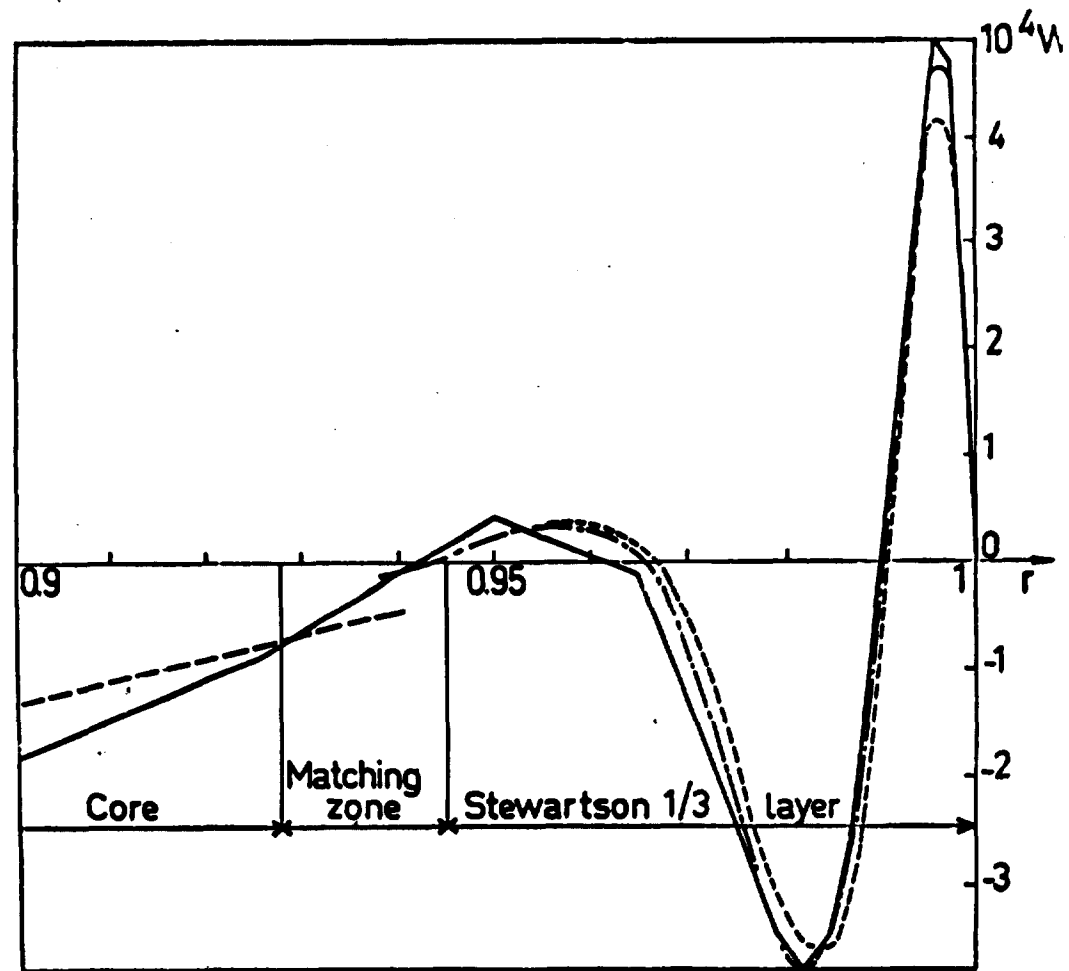


FIG 7 : Axial velocity profile near the wall in the mid plane,  $Z = 0$

Antisymmetric case A

— CENTAURE CODE

- - - Stewartson 1/3 layer 2 terms  $w^{(0)} + \epsilon^{1/3} w^{(1)}$

--- Stewartson 1/3 layer 1 term  $w^{(0)}$

--- Core solution

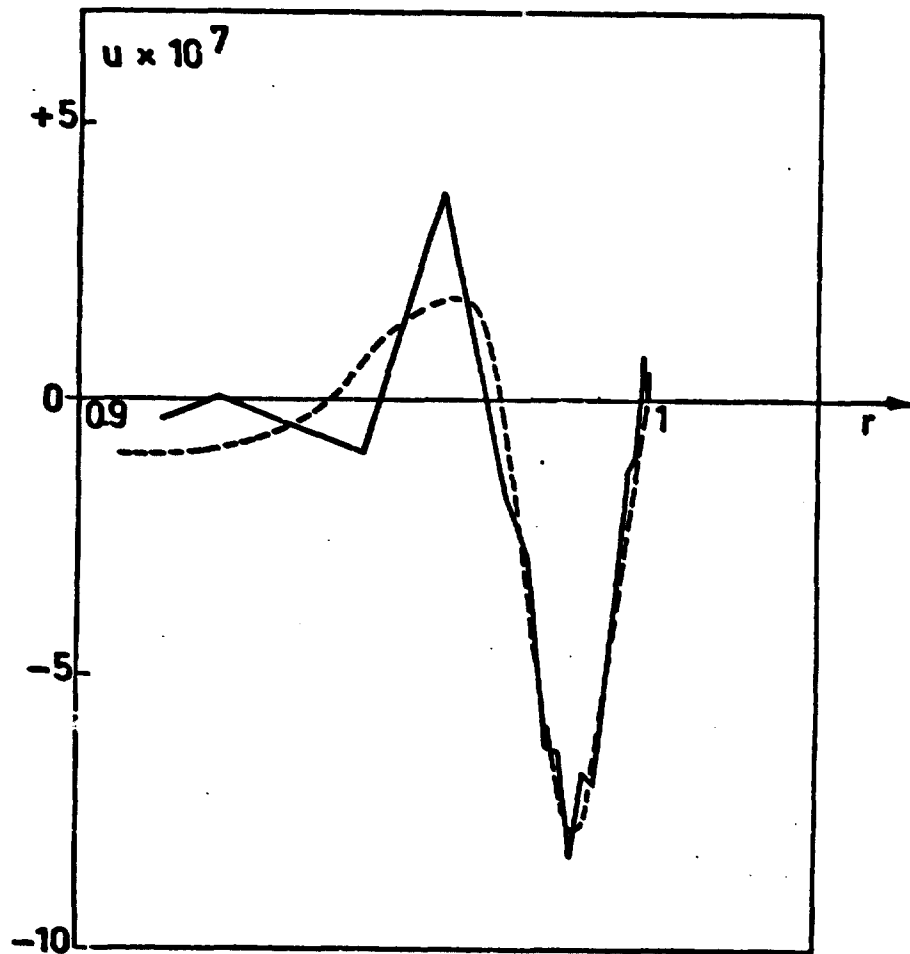


FIG 8 : Radial velocity in the Stewartson 1/3 layer  
 Antisymmetric case A,  $z = 0.6\beta$   
 — CENTAURE CODE  
 ---- Matched asymptotic expansions

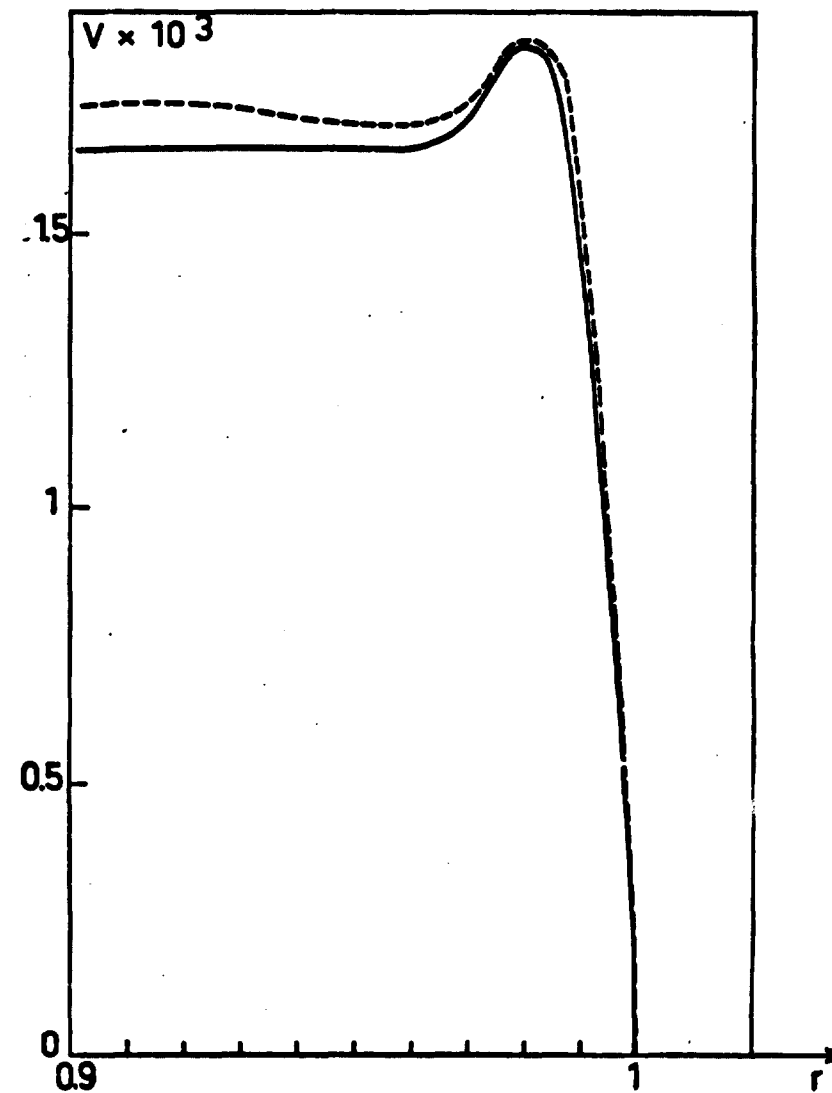


FIG 9 : Azimuthal velocity in the Stewartson 1/3 layer  
 Antisymmetric case A,  $z = 0.6\beta$   
 — CENTAURE CODE  
 ----  $v^{(2)}, \epsilon^{1/6} v^{(1)}$  Matched asymptotic expansions

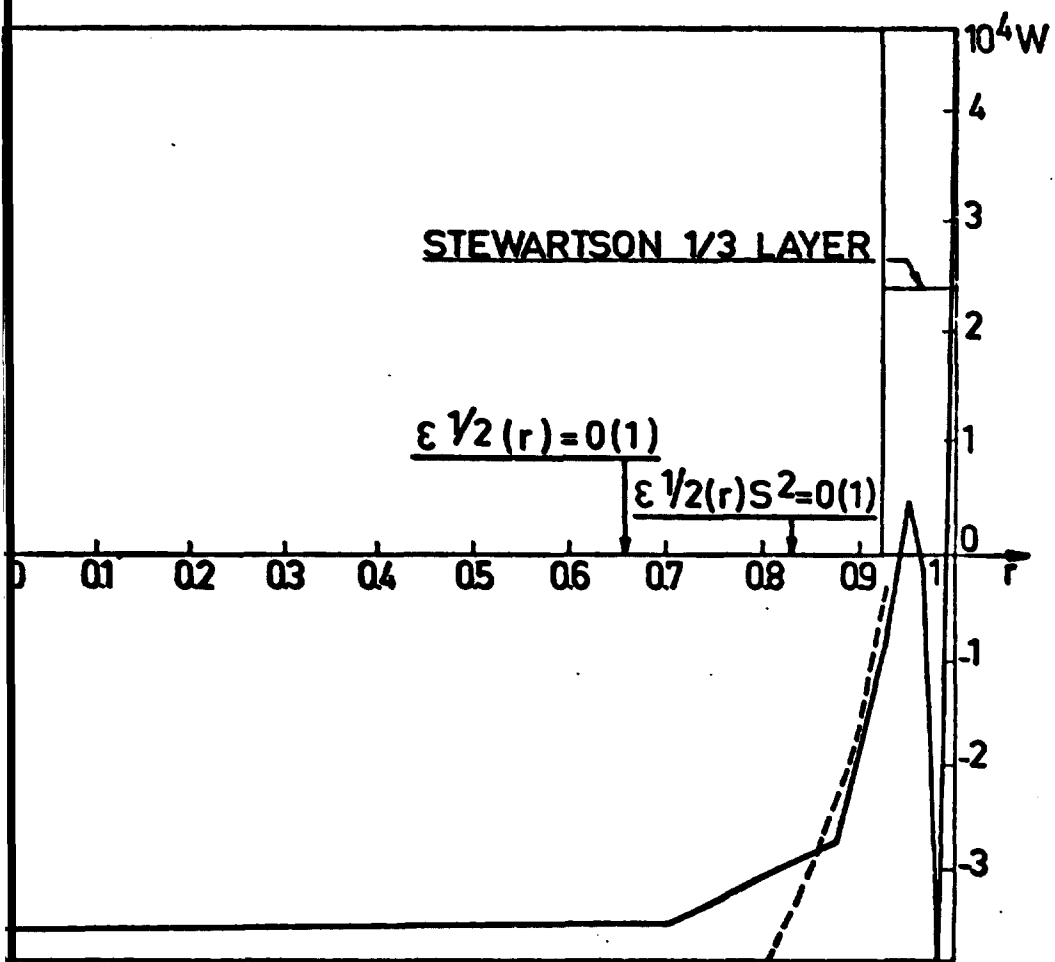


FIG 10: Axial velocity in the core - Antisymmetric case A,  $z = 0.5\delta$

— CENTAURE CODE  
 ---- Core solution (non viscous)

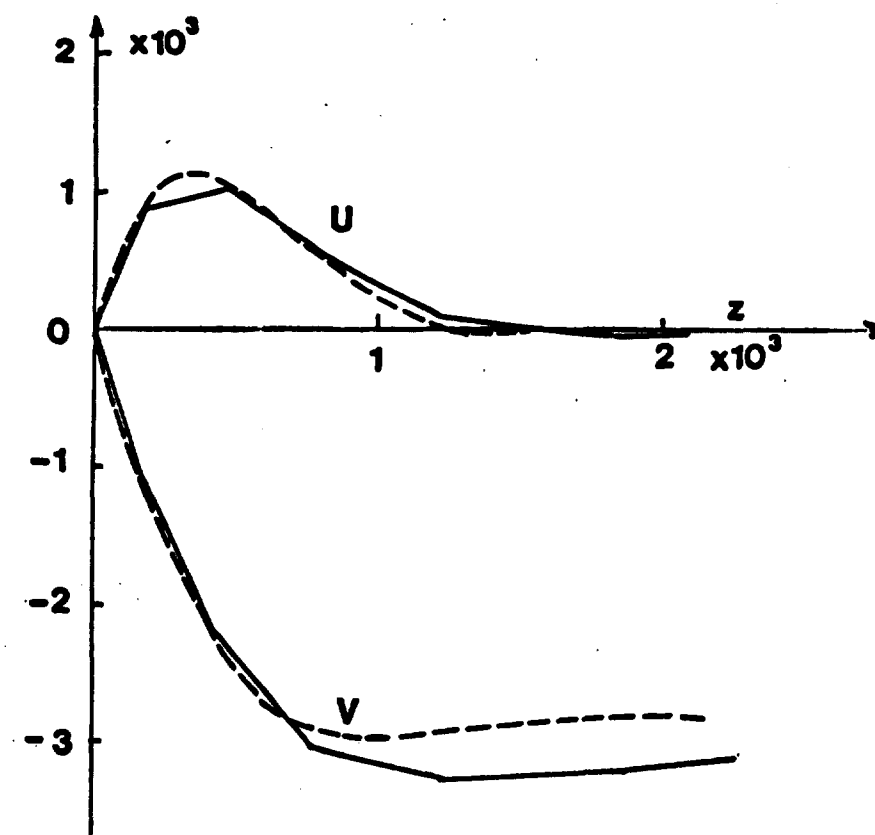


FIG 11: Radial and azimuthal velocity profiles in the Ekman layer.

Antisymmetric case A -  $r = 0.875$   
 — CENTAURE CODE  
 ---- Boundary layer solution

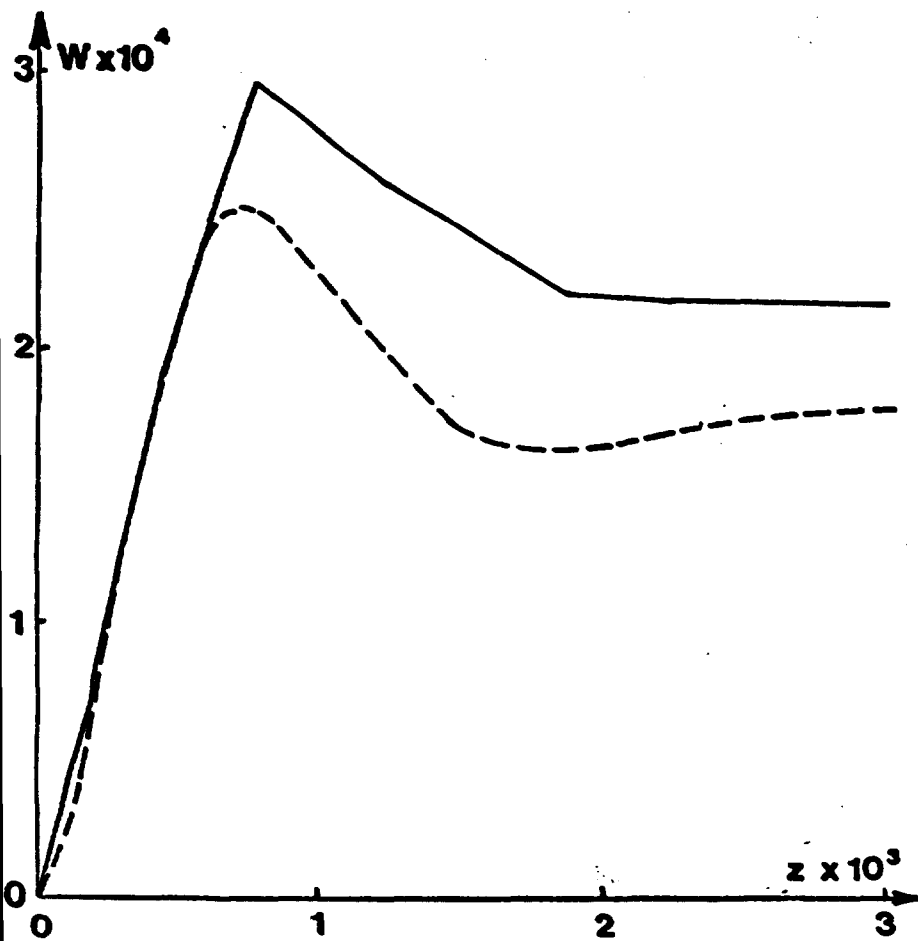


FIG 12: Axial velocity profile in the Ekman layer  
 Antisymmetric case A -  $r = 0.875$   
 — CENTAURE CODE  
 ---- Boundary layer solution

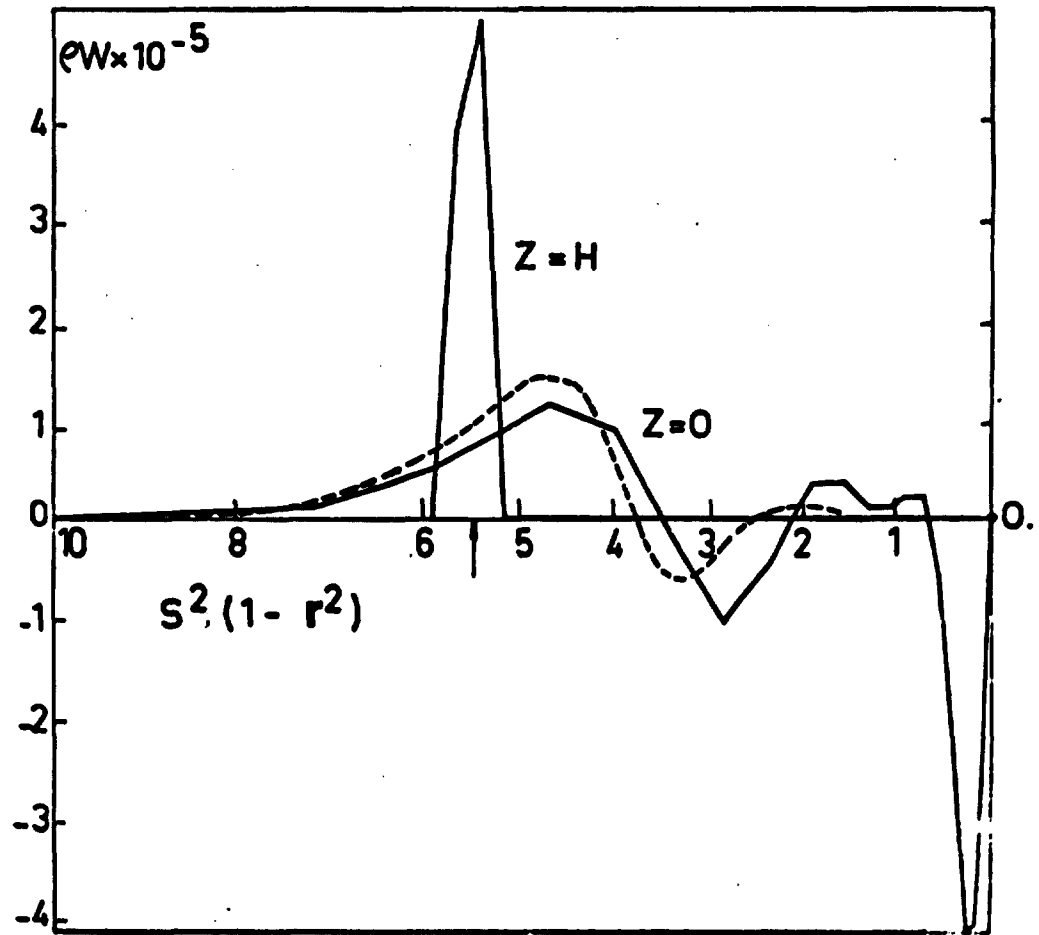


FIG 13: Mass velocity profile in detached 1/3 layer;  $S^2 = 32$ ; case B  
 — CENTAURE CODE  
 ---- ASYMPTOTIC EXPANSIONS - LOUVET (1976)

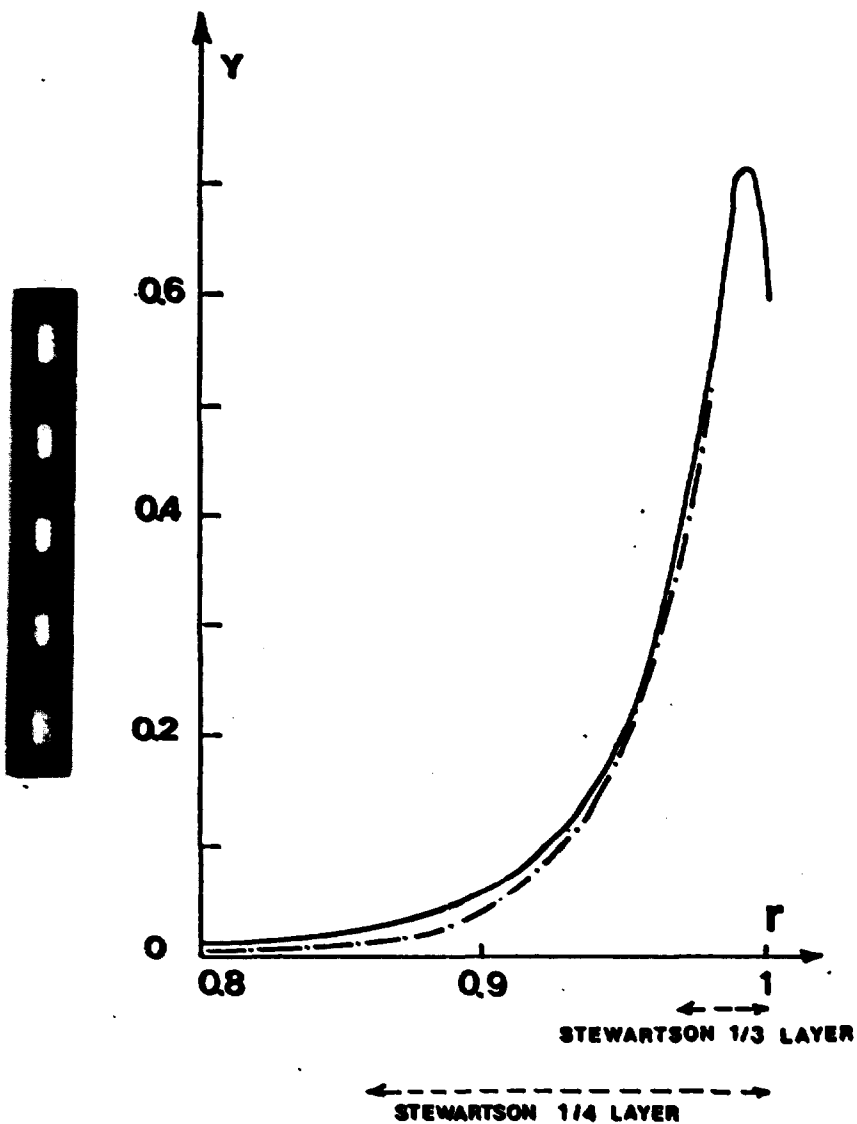


FIG 14: Variation of the thermal wind quantity in the Stewartson 1/3 and 1/4 layers - Symmetric case C -  $Z = 0.64 \beta$   
 — CENTAURE CODE  
 - - - Asymptotic expansions

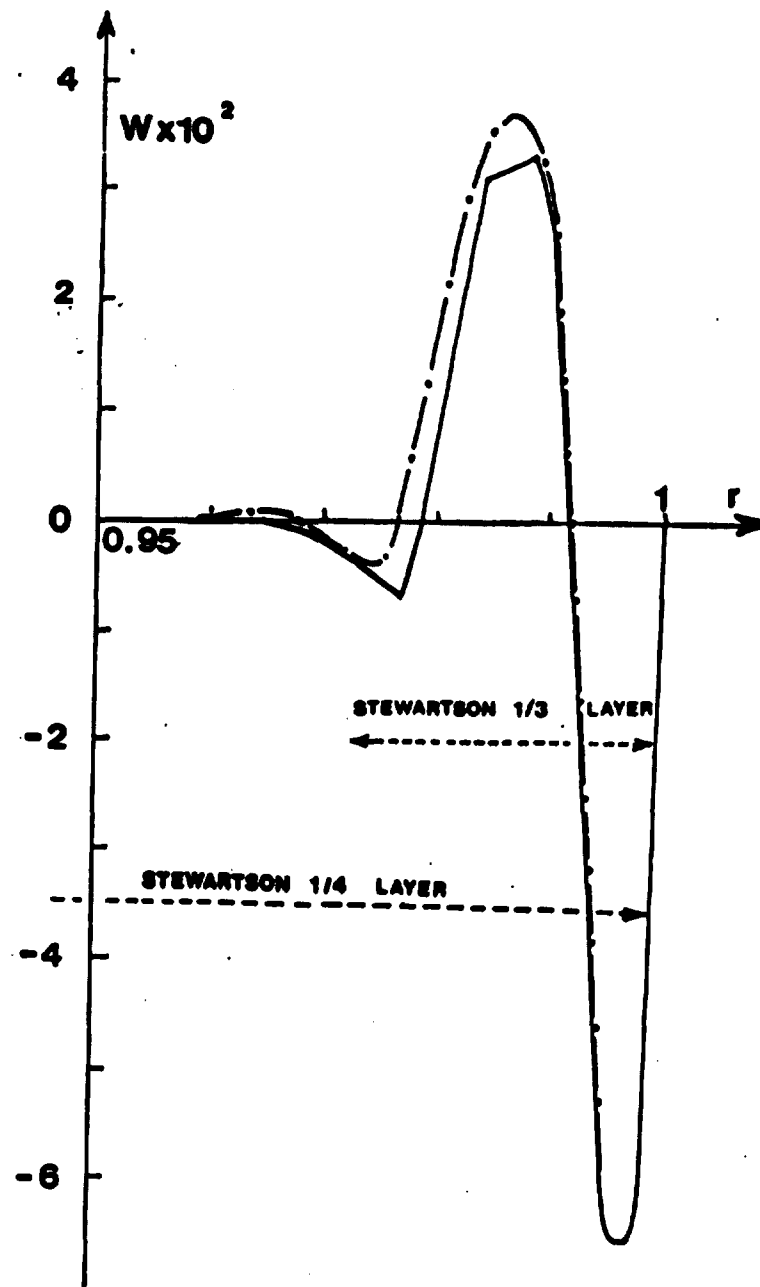


FIG 15: Axial velocity profile in the Stewartson 1/3 and 1/4 layers. Symmetric case C -  $Z = 0.64 \beta$   
 — CENTAURE CODE  
 - - - Asymptotic expansions